Clock Timing Mismatch Compensation in Direct Sampling Receiver

Manabu Sakai, Hai Lin, Katsumi Yamashita
Graudate School of Engineering
Osaka Prefecture Univeristy
Sakai, Osaka 599-8531, Japan
Email: {ss106025@edu, lin@eis, yamashita@eis}.osakafu-u.ac.jp

Jingxian Wu
Department of Electrical Engineering
University of Arkansas
Fayetteville, AR 72701, USA
Email: wuj@uark.edu

***Abstract*—In this paper, we study the impact of clock timing mismatch of analog-to-digital converter in a receiver that employs quadrature bandpass sampling of the radio frequency (RF) signal. It is shown that the clock timing mismatch introduces not only symbol timing offset but also image interference, that is, the interference between in-phase and quadrature signals. Then, a mismatch compensation scheme and a pilot-aided mismatch estimation method are proposed. We also propose a blind estimation method, where the clock timing mismatch can be estimated from the second order statistics of the sampled sequences. Numerical simulations confirm the validity of the proposed methods, even in the presence of unknown channel.**

***Keywords*—Direct sampling receiver, bandpass sampling, clock timing mismatch estimation**

I. Introduction

Nowadays, there exist various wireless communication standards, and it is expected that a wireless transceiver can be readily adapted to these standards. Software defined radio (SDR) is considered as a promising solution to realize such reconfigurable radio transceivers [1]. In an SDR receiver, analog circuits are desired to be mitigated into the digital domain as much as possible, and consequently, the received signal is preferred to be directly sampled just behind the receive antenna. Considering the high frequency of the received RF signal, a very high speed analog-to-digital converter (ADC) is required to sample it at Nyquist rate. However, the state-of-the-art ADC satisfying this requirement is not only expensive but also high power-consumption. As long as the conveyed baseband signal is our concern, an effective way is to directly sample the received RF signal at sub-Nyquist rate, namely, bandpass sampling [2].

By saving one ADC and one local oscillator (LO) in exchange for one bandpass filter to eliminate out-of-band signals, the direct sampling receiver makes itself a competitive alternative to the well-known direct conversion receiver (DCR). In the context of bandpass sampling, the RF signal can be downconverted into an inter-mediate frequency (IF) band by *uniformly* sampling at sub-Nyquist rate that is carefully chosen to avoid aliasing, and subsequently, the IF signal is digitally downconverted into the baseband [2], [3], [4]. A further drop in sampling rate can be achieved by periodic *non-uniform* bandpass sampling [5], [6], which is also known as quadrature bandpass sampling and a specific type of the Kohlenberg's second order sampling [7]. Different from uniform bandpass sampling, quadrature bandpass sampling allows two aliased bands to overlap with each other, since the appropriately allocated non-uniform clock plays a role as Hilbert transform. When the carrier frequency of the received RF signal is an integer multiple of sampling frequency, the aliased spectrum is centered at zero, the baseband signal can be directly obtained from the output of the ADC. Obviously, the ADC is the key device in a direct sampling receiver, and the signal quality highly depends on the accuracy of its clock timing. The effect of ADC clock jitter in uniform and non-uniform bandpass sampling can be found in [8], [9] and [10], respectively. For non-uniform bandpass sampling, the clock signal is exactly composed of two uniform clock signals with an intentional timing offset. This timing offset is used to obtain a timing-shifted quadrature-phase signal first, then a subsequent digital timing offset correction provides the proper quadrature-phase signal [11]. Since the timing offset is inversely proportional to the carrier frequency, a precise offset is not easy to achieve in practice. Although it is known that an incorrect offset, namely a clock timing mismatch (CTM), will cause severe signal degradation [12], how to estimate it is still unclear.

In this paper, we focus on the CTM compensation in receivers which employ quadrature bandpass sampling. First, we formulate the mathematical model of quadrature bandpass sampling with incorrect clock timing offset. It is shown that the CTM introduces not only symbol timing offset but also cross-talk between the in-phase and quadrature-phase signals, that is to say, image interference. Thus, the effect of CTM can be analyzed in terms of image rejection ratio (IRR). It can be found that the IRR is very sensitive to the CTM, and the range of tolerable mismatch in practice is given. Then, a compensation scheme is introduced, and a CTM estimation method is proposed. Since the samples at the ADC output are also distorted by the symbol timing offset, the estimation of CTM is not straightforward, even with the assistance of pilot. Fortunately, considering the practical CTM value, we find that the symbol timing offset is negligible small compared to the symbol duration. Based on this observation, a pilot-aided CTM estimation method is proposed. Also, we propose a blind CTM estimation method, where the CTM is estimated from the auto- and cross-correlation of the sampled sequences. Finally, the

validity of the proposed methods are confirmed by numerical simulations.

II. Problem Formulation

A. Quadrature Bandpass Sampling

We assume that the signal of interest lies in $[f_c - B/2, f_c + B/2] \cup [-f_c - B/2, -f_c + B/2]$, where f_c and B denote the carrier frequency and the bandwidth of the signal, respectively. To avoid aliasing, the received signal is preliminarily filtered by a bandpass filter, which strictly eliminates out-of-band signals. As a consequence, the bandpass signal contains no spectrum except for $[f_c - B/2, f_c + B/2] \cup [-f_c - B/2, -f_c + B/2]$, which can be represented as

$$\begin{aligned} x_p(t) &= x_I(t)\cos(2\pi f_c t) - x_Q(t)\sin(2\pi f_c t) \\ &= \frac{1}{2}[x(t)e^{j2\pi f_c t} + x^*(t)e^{-j2\pi f_c t}], \end{aligned} \tag{1}$$

where $x(t) = x_I(t) + jx_Q(t)$ is the baseband representation of $x_p(t)$.

In quadrature bandpass sampling, $x_p(t)$ is directly sampled at a sub-Nyquist rate. The sampling interval T_s is chosen to satisfy $\mathrm{mod}(T_s, 1/f_c) = 0$, and $T_s \leq 1/B$. If the carrier frequency f_c is an integer multiple of B, which is called as half-integer positioning [2], then the sampling interval becomes $1/B$. In this paper, half-integer positioning is assumed for the sake of simplicity, that is, $T_s = 1/B$ and $f_c T_s = P$, where P is an arbitrary integer. Noteworthy, even if the band of signal is not half-integer positioning, the following discussion can be applied by relaxing the sampling interval to $T_s < 1/B$ and subsequently employing the digital sampling-rate conversion.

The ADC employs a non-uniform sampling clock, which can be obtained from the system clock using a programmable divider. Then, under the assumption of perfect carrier synchronization, the received RF signal is sampled at $t = nT_s$ and $t = nT_s + \Delta T$, respectively, where ΔT denotes the intentional timing offset. The sampled sequence at $t = nT_s$ can be written as

$$\begin{aligned} x_1(n) &= x_p(nT_s) \\ &= \frac{1}{2}[x(nT_s)e^{j2\pi f_c nT_s} + x^*(nT_s)e^{-j2\pi f_c nT_s}] \\ &= \frac{1}{2}[x(nT_s) + x^*(nT_s)] = x_I(nT_s). \end{aligned} \tag{2}$$

On the other hand, let the timing offset be

$$\Delta T = \frac{3}{4f_c} + LT_s, \tag{3}$$

where L is an arbitrary integer, then the sampled sequence at $t = nT_s + \Delta T$ is given by

$$\begin{aligned} x_2(n) &= x_p(nT_s + \Delta T) \\ &= \frac{1}{2}[x(nT_s + \Delta T)e^{j2\pi f_c nT_s}e^{j2\pi f_c \Delta T} \\ &\quad + x^*(nT_s + \Delta T)e^{-j2\pi f_c nT_s}e^{-j2\pi f_c \Delta T}] \\ &= \frac{1}{2}[-jx(nT_s + \Delta T) + jx^*(nT_s + \Delta T)] \\ &= x_Q(nT_s + \Delta T). \end{aligned} \tag{4}$$

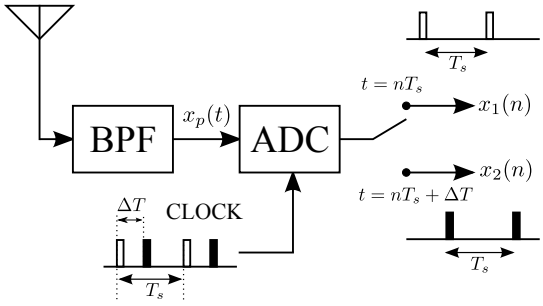

Fig. 1. Diagram of quadrature bandpass sampling.

Therefore, we can obtain the baseband equivalent of $x_p(t)$ as

$$x(n) = x_1(n) + j\mathbf{x}_2(n)\mathbf{g}^T \tag{5}$$

where $\mathbf{x}_2(n) = [x_2(n), \ldots, x_2(n - K + 1)]$, and $\mathbf{g}$ is a compensation filter for the distortion caused by the symbol timing offset ΔT. Since ΔT is obviously fractional to the sampling interval, one possible choice of $\mathbf{g}$ is a fractional delay filtering [13] with finite impulse response (FIR) given by

$$g(k) = \begin{cases} \mathrm{sinc}(k - \Delta T/T_s), & 0 \leq k \leq K - 1 \\ 0, & \text{otherwise} \end{cases}, \tag{6}$$

where $K = 2L + 1$ denotes the filter length. As we can see from (6), the length of the filter $\mathbf{g}$ is very long, due to the long tail of sinc function. Therefore, we need to the impulse response up to KT_s, which is chosen as the impulse response converges to some extent. The effect of this truncation will be examined later by numerical simulations. Once the timing offset induced distortion is perfectly compensated, we have the desired baseband signal

$$x(n) = x_I(nT_s) + jx_Q(nT_s).$$

Fig. 1 shows a diagram of quadrature bandpass sampling in the direct sampling receiver.

B. Clock Timing Mismatch

Since $f_c T_s = P$, the timing offset in (3) can be rewritten as

$$\Delta T = \frac{3}{4f_c} + \frac{LP}{f_c} = \left(\frac{3}{4} + LP\right)\frac{1}{f_c}. \tag{7}$$

It is clear that the timing offset is inversely proportional to the carrier frequency. Although the sampling interval T_s has been relaxed to P/f_c, the timing offset still contains a fractional part of $1/f_c$, which is not easy to achieve in practice.

When the clock timing offset is incorrect, even with perfect samples of $x_1(n) = x_p(nT_s) = x_I(nT_s)$, $x_2(n)$ is however obtained by sampling $x_p(t)$ at $t = nT_s + \Delta T + \phi$, where ϕ denote a CTM. The corresponding sequence is given by

$$\begin{aligned} x_2'(n) &= x_p(nT_s + \Delta T + \phi) \\ &= \frac{1}{2}[-jx(nT_s + \Delta T + \phi)e^{j2\pi f_c \phi} \\ &\quad + jx^*(nT_s + \Delta T + \phi)e^{-j2\pi f_c \phi}] \\ &= x_Q(nT_s + \Delta T + \phi)\cos(2\pi f_c \phi) \\ &\quad + x_I(nT_s + \Delta T + \phi)\sin(2\pi f_c \phi). \end{aligned} \tag{8}$$

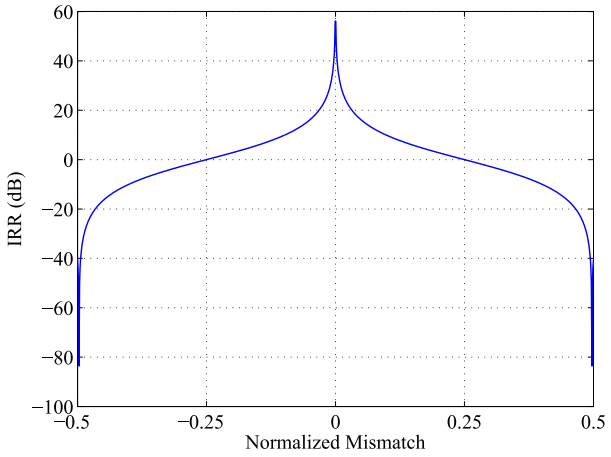

Fig. 2. IRR of the received signal at normalized frequency $f/f_s = 0.3$ when the CTM ϕ is varied from $-1/2f_c$ to $1/2f_c$.The carrier frequency is assumed to be $f_c = 50f_s$.

Compared to (4), we can see that the CTM brings not only an extra symbol timing offset but also part of in-phase signal to the quadrature-phase signal. The effect of the CTM can be observed more clearly from the frequency domain. Given $\mathbf{x}_2'(n) = [x_2'(n), \ldots, x_2'(n-K+1)]$, let

$$x'(n) = x_1(n) + j\mathbf{x}_2'(n)\mathbf{g}^T, \tag{9}$$

whose frequency domain representation is

$$\begin{aligned} X'(f)=&\frac{1}{2}[1+e^{j2\pi(f(\Delta T+\phi)/T_s+f_c\phi)}G(f)]X(f) \\ &+\frac{1}{2}[1-e^{j2\pi(f(\Delta T+\phi)/T_s-f_c\phi)}G(f)]X^*(-f), \end{aligned} \tag{10}$$

where $X'(f)$, $X(f)$, and $G(f)$ represent the Fourier transform of $x'(n)$, $x(n)$, and $\mathbf{g}$, respectively. With an ideal compensation filter of $G(f) = e^{-j2\pi f\Delta T/T_s}$, we obtain

$$X'(f) = A_1(f)X(f) + A_2(f)X^*(-f), \tag{11}$$

where,

$$A_1(f)=\frac{1}{2}[1+e^{j2\pi(f\phi/T_s+f_c\phi)}], \tag{12}$$

$$A_2(f)=\frac{1}{2}[1-e^{j2\pi(f\phi/T_s-f_c\phi)}]. \tag{13}$$

From (11), we can see that the CTM results at an image interference, therefore the IRR is a good measurement of its effect, which is given by

$$IRR(f) = \frac{|A_1(f)|^2}{|A_2(f)|^2}. \tag{14}$$

Fig. 2 shows the IRR versus the CTM for $-1/2f_c$ to $1/2f_c$. It can be seen that the IRR curve is very sharp around the origin, which means even a small CTM can cause severe distortion. In case of $\phi = \pm 1/4f_c$, the IRR becomes 0 dB, which corresponds to the complete loss of the quadrature-phase signal, and there is no way to recover it. As a consequence, the tolerable timing mismatch in practice is limited to $(-1/4f_c, 1/4f_c)$.

III. Mismatch Compensation

Obviously, the CTM should be compensated before any further processing. If the CTM ϕ is known, the sample timing offset in $x_2'(n)$ can be easily compensated by replacing ΔT with $\Delta T + \phi$ in the compensation filter $\mathbf{g}$ of (5). After perfect symbol timing offset compensation, the output signal is given by

$$\bar{x}_2'(n) = x_Q(nT_s)\cos(2\pi f_c\phi) + x_I(nT_s)\sin(2\pi f_c\phi). \tag{15}$$

The remaining cross-talk in (15) is similar to the effect of IQ imbalance in the DCR, which can be compensated as

$$\hat{x}_I(n)=x_1(n), \tag{16}$$

$$\hat{x}_Q(n)=\cot(2\pi f_c\phi)\bar{x}_2'(n) - \tan(2\pi f_c\phi)x_1(n). \tag{17}$$

A. Pilot-aided Mismatch Estimation

To implement the above-mentioned compensation scheme, we need to estimate the CTM first. Although the CTM is contained in the Q branch symbols in (8), it seems not easy to obtain it even $x_I(nT_s+\Delta T)$ and $x_Q(nT_s+\Delta T)$ are known for a calibration case, since the unknown CTM ϕ actually result in unknown $x_I(nT_s+\Delta T+\phi)$ and $x_Q(nT_s+\Delta T+\phi)$. The effect of ϕ should be investigated in more details.

Considering the range of tolerable ϕ, the symbol timing offset $\Delta T + \phi$ satisfies

$$\left(\frac{1}{2f_cT_s}+L\right)T_s \le \Delta T+\phi \le \left(\frac{1}{f_cT_s}+L\right)T_s, \tag{18}$$

where the symbol timing offset is separated into an integer part and a fractional part with respect to the sampling interval T_s, for the sake of clarity. Since L and P are integer, the fractional part becomes

$$\frac{T_s}{2P} \le \Delta T+\phi-LT_s \le \frac{T_s}{P}. \tag{19}$$

Since the carrier frequency is usually much higher than the sampling frequency, P is a large number and the fractional part of ϕ is quite small with respect to T_s. For example, if the signal bandwidth is $B = 20$ MHz and the carrier frequency is $f_c = 1$ GHz, then $P = 50$ and $1/P = 0.02 \ll 1$, which means the fractional part is less than 2% of the sampling interval. Bearing in mind that the baseband signal is generally a low-pass signal, the effect of this small fractional part of timing offset is negligible. Therefore, we can approximate that $x(nT_s + \Delta T + \phi) \approx x(nT_s + LT_s)$. This observation is the key for the estimation of ϕ, since L is a known design parameter, and the corresponding integer timing offset can be easily handled by realigning two branch signals.

Using the approximation, (8) can be reduced to

$$x_2'(n) = x_Q(n+L)\cos(2\pi f_c\phi)+x_I(n+L)\sin(2\pi f_c\phi). \tag{20}$$

Even with known pilot sequence, since the received signal $x_I(n)$ and $x_Q(n)$ are usually distorted by the channel, it is not easy to estimate the mismatch directly from (20) when the channel response is unknown. However, it can be seen that the mismatch ϕ is independent of the time index n, therefore,

the periodic pilot sequence is suitable. Here, we employ the generalized periodic pilot (GPP) sequence in [14] to estimate the CTM. The GPP sequence $\mathbf{x}(n) = [x(n)\, x(n-1)\, \ldots\, x(n-M+1)]^T$ is designed to satisfy $\mathbf{x}(n+Q) = e^{j\theta}\mathbf{x}(n)$, where Q denotes the period of GPP and θ is an intentional phase rotation. This relationship still holds after passing through the linear time-invariant channel whenever the channel length is less than Q. From (16) and (17), the received sequence after the compensation can be written as

$$\bar{\mathbf{x}}(n) = \mathbf{x}_1(n+L) + j\{\beta\mathbf{x}_2'(n) - \alpha\mathbf{x}_1(n+L)\}, \quad (21)$$

where, $\alpha = \tan(2\pi f_c\phi)$, $\beta = 1/\cos(2\pi f_c\phi)$, and $\mathbf{x}_1(n)$ and $\mathbf{x}_2'(n)$ are the vector representation of $x_1(n)$ and $x_2'(n)$, respectively. The compensated GPP sequence should also satisfy $\bar{\mathbf{x}}(n+Q) - e^{j\theta}\bar{\mathbf{x}}(n) = 0$, and after simplifying the equation, we obtain

$$\mathbf{A}\mathbf{h} = \mathbf{b}, \quad (22)$$

where $\mathbf{h} = [\cos\theta + \alpha\sin\theta, \cos\theta - \alpha\sin\theta, \beta\sin\theta]^T$, $\mathbf{b} = [\mathbf{x}_1^T(n+L+Q), \mathbf{x}_1^T(n+L)]^T$, and

$$\mathbf{A} = \begin{bmatrix} \mathbf{x}_1(n+L) & \mathbf{0} & -\mathbf{x}_2'(n) \\ \mathbf{0} & \mathbf{x}_1(n+L+Q) & \mathbf{x}_2'(n+Q) \end{bmatrix}, \quad (23)$$

respectively. (22) can be solved based on least square (LS) criterion, then we have

$$\hat{\phi} = \left(\frac{1}{2\pi f_c}\right)\tan^{-1}\left(\frac{\hat{\mathbf{h}}(1) - \hat{\mathbf{h}}(2)}{2\sin\theta}\right). \quad (24)$$

where,

$$\hat{\mathbf{h}} = (\mathbf{A}^T\mathbf{A})^{-1}\mathbf{A}^T\mathbf{b}. \quad (25)$$

B. Blind Mismatch Estimation

Compared to the pilot-aided estimation, blind estimation methods have the advantage of effective resource utilization by reducing excess pilot sequences and the independency of the standards. In this section, we also propose a blind estimation method using the second order statistics of the received signals.

Under the assumption of perfect carrier synchronization, the autocorrelation function (ACF) of $x_I(n)$ can be obtained from $x_1(n)$ as

$$R_{x_1}(k) = \mathbb{E}[x_1(n)x_1(n-k)] = \mathbb{E}[x_I(n)x_I(n-k)] = R_{x_I}(k) \quad (26)$$

where $\mathbb{E}[\cdot]$ denotes expectation. On the other hand, using the approximation in (20), the cross-correlation function (CCF) of $x_1(n)$ and $x_2'(n)$ is given by

$$\begin{aligned} R_{x_{12'}}(k) &= \mathbb{E}[x_1(n)x_2'(n-k)] \\ &= \cos(2\pi f_c\phi)\mathbb{E}[x_I(n)x_Q(n-k+L)] \\ &\quad + \sin(2\pi f_c\phi)\mathbb{E}[x_I(n)x_I(n-k+L)]. \end{aligned} \quad (27)$$

It is known that the signal employed in various wireless communication standards, such as QAM or OFDM signal, is *proper* [15], which means that the CCF of its in-phase and quadrature-phase signals obeys

$$R_{x_{IQ}}(k) = \mathbb{E}[x_I(n)x_Q(n-k)] = 0, \quad \forall k \in \mathbb{R}. \quad (28)$$

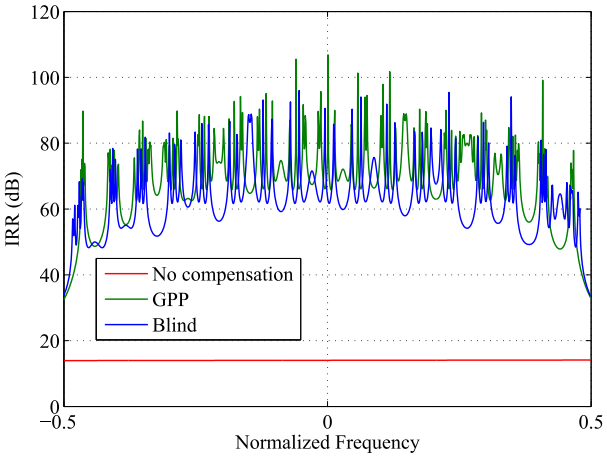

Fig. 3. IRR under AWGN channel, SNR=30 dB, $\phi = -1/16f_c$.

Since this proper property holds after passing through the channel, (27) can be reduced to

$$R_{x_{12'}}(k) = \sin(2\pi f_c\phi)R_{x_I}(k-L). \quad (29)$$

Then, the CTM ϕ can be estimated as

$$\hat{\phi} = \left(\frac{1}{2\pi f_c}\right)\sin^{-1}\left(\frac{R_{x_{12'}}(k)}{R_{x_1}(k-L)}\right), \quad (30)$$

where $R_{x_I}(k-L)$ can be obtained using $x_1(n)$ in (26).

IV. Numerical Simulation

The proposed methods are evaluated through numerical simulations. In the following simulations, the signal is OFDM signal with 1024 subcarriers, whose spacing is 15 kHz and each subcarrier is modulated by 64-QAM. We assume the half-integer positioning for the spectrum location and the carrier frequency is set to be 50 times higher than the sampling frequency, that is, $P = 50$, and the length of $\mathbf{g}$ is $K = 17$. The multi-path fading channel has 6 paths, and the power delay profile is based on ITU Pedestrian B channel model. The length of the cyclic prefix is 64, and the period of GPP sequence is $Q = 64$ and $\theta = \pi/8$. While $M = 600$ samples of GPP sequence are used in the pilot-aided estimation, the blind estimation method utilizes 10 OFDM symbols.

Fig. 3 and 4 show the IRR performances of the proposed methods in AWGN channel and multi-path fading channel, respectively. It can be seen that the pilot-aided estimation improves the IRR across the signal band, which achieves near 80 dB IRR for both AWGN and multi-path fading channels. On the other hand, the blind estimation method also shows near 70 dB IRR, that is about 50 dB above the no compensation case. We also evaluate the symbol error rate (SER) of the proposed method under multi-path fading channel. Fig. 5 shows SER performance versus SNR after the compensation of the clock timing mismatch. The CTM is uniformly distributed in $(-1/8f_c, 1/8f_c)$ corresponds to above 7 dB IRR. The SER of the DCR is plotted together as a benchmark. While the error floor can be seen in the no

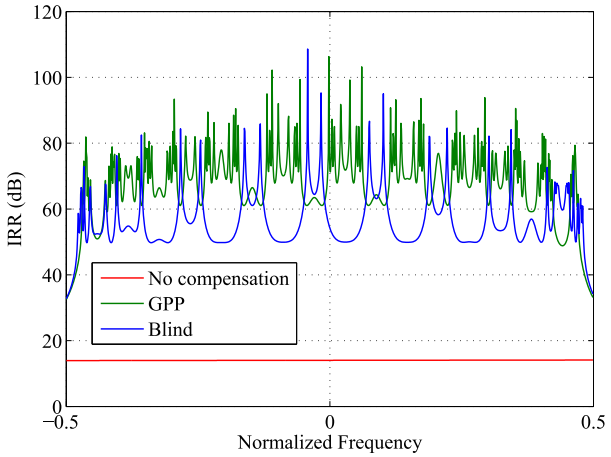

Fig. 4. IRR under multi-path fading channel, SNR=30 dB, $\phi = -1/16 f_c$.

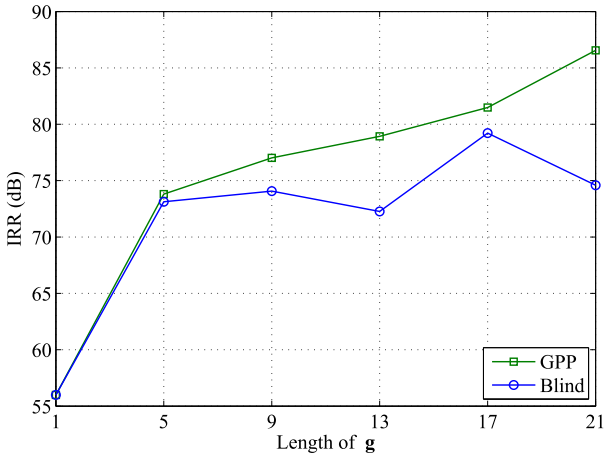

Fig. 6. IRR versus length of $\mathbf{g}$, SNR=30 dB, $\phi = -1/16 f_c$.

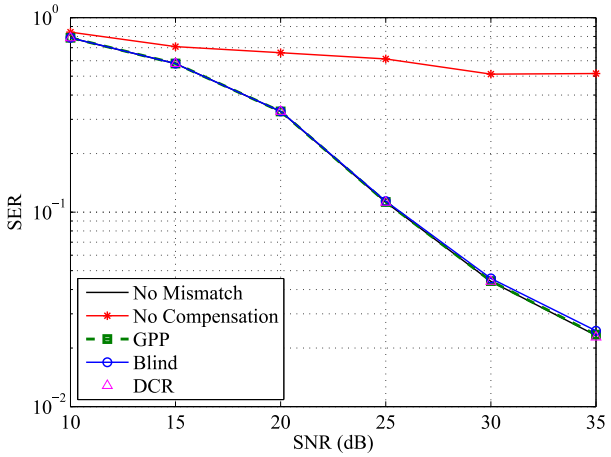

Fig. 5. SER performance of the proposed methods.

compensation case, both of the pilot-aided and blind estimation method show good SERs very close to the ideal case of no mismatch, as well as the DCR.

Since the compensation filter $\mathbf{g}$ originally has a long impulse response due to the slow convergence of sinc function, its truncation effect should be investigated in detail. Fig. 6 shows the average IRR over signal bandwidth under various length of $\mathbf{g}$. It can be seen that $K = 17$ is sufficient for the compensation, which brings around 80 dB IRR.

V. Conclusion

In this paper, we focused on the clock timing mismatch in quadrature bandpass sampling based direct sampling receiver, and showed that it introduces not only symbol timing offset but also image interference. We analyzed the effect of clock timing mismatch and found that the image rejection ratio is quite sensitive to the mismatch. The tolerable range of mismatch was given, then the compensation scheme and pilot-aided and blind estimation method were proposed using an approximation of the timing-shifted quadrature-phase signal. The performance of the proposed method was evaluated by the numerical simulations and its satisfactory image rejection ratio and symbol error rate performance were demonstrated.

References

[1] B. Almeroth, S. Krone, and G. Fettweis, "Analyzing the signal-to-noise ratio of direct sampling receivers," in *Proc. IEEE Int. Conf. Commun. (ICC)*, June 2013, pp. 4561–4565.

[2] R. Vaughan, N. Scott, and D. White, "The theory of bandpass sampling," *IEEE Trans. Signal Process.*, vol. 39, no. 9, pp. 1973–1984, Sep. 1991.

[3] C.-H. Tseng and S.-C. Chou, "Direct downconversion of multiband RF signals using bandpass sampling," *IEEE Trans. Wireless Commun.*, vol. 5, no. 1, pp. 72–76, Jan. 2006.

[4] Y.-P. Lin, Y.-D. Liu, and S.-M. Phoong, "A new iterative algorithm for finding the minimum sampling frequency of multiband signals," *IEEE Trans. Signal Process.*, vol. 58, no. 10, pp. 5446–5450, Oct. 2010.

[5] Y.-P. Lin and P. Vaidyanathan, "Periodically nonuniform sampling of bandpass signals," *IEEE Trans. Circuits Syst. II, Analog Digit. Signal Process.*, vol. 45, no. 3, pp. 340–351, Mar. 1998.

[6] A. Dempster, "Quadrature bandpass sampling rules for single- and multiband communications and satellite navigation receivers," *IEEE Trans. Aerosp. Electron. Syst.*, vol. 47, no. 4, pp. 2308–2316, Oct. 2011.

[7] A. Kohlenberg, "Exact interpolation of band-limited functions," *Journal of Applied Physics*, vol. 24, no. 12, pp. 1432–1436, 1953.

[8] V. Syrjala and M. Valkama, "Jitter mitigation in high-frequency bandpass-sampling ofdm radios," in *Proc. IEEE Wireless Commun. Networking Conf. (WCNC)*, 2009.

[9] G. Fudge, H. Azzo, and F. Boyle, "A reconfigurable direct RF receiver with jitter analysis and applications," *IEEE Trans. Circuits Syst. I, Reg. Papers*, vol. 60, no. 7, pp. 1702–1711, July 2013.

[10] M. Inamori, A. Bostamam, and Y. Sanada, "Influence of timing jitter on quadrature charge sampling," *IET Commun.*, vol. 1, no. 4, pp. 705–710, Aug. 2007.

[11] M. Valkama and M. Renfors, "A novel image rejection architecture for quadrature radio receivers," *IEEE Trans. Circuits Syst. II, Exp. Briefs*, vol. 51, no. 2, pp. 61–68, Feb. 2004.

[12] S. Karvonen, T. Riley, and J. Kostamovaara, "A CMOS quadrature charge-domain sampling circuit with 66-dB SFDR up to 100 MHz," *IEEE Trans. Circuits Syst. I, Reg. Papers*, vol. 52, no. 2, pp. 292–304, Feb. 2005.

[13] T. Laakso, V. Valimaki, M. Karjalainen, and U. Laine, "Splitting the unit delay," *IEEE Signal Process. Mag.*, vol. 13, no. 1, pp. 30–60, Jan. 1996.

[14] H. Lin, X. Zhu, and K. Yamashita, "Low-complexity pilot-aided compensation for carrier frequency offset and I/Q imbalance," *IEEE Trans. Commun.*, vol. 58, no. 2, pp. 448–452, Feb. 2010.

[15] L. Anttila, M. Valkama, and M. Renfors, "Circularity-based I/Q imbalance compensation in wideband direct-conversion receivers," *IEEE Trans. Veh. Technol.*, vol. 57, no. 4, pp. 2099–2113, July 2008.